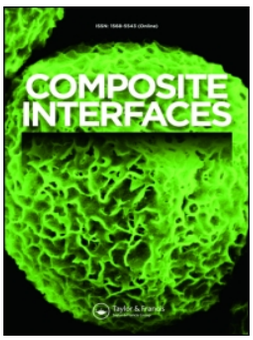

Composite Interfaces

ISSN: 0927-6440 (Print) 1568-5543 (Online) Journal homepage: http://www.tandfonline.com/loi/tcoi20

Efficient dispersion of carbon nanotube by synergistic effects of sisal cellulose nano-fiber and graphene oxide

Zihao Xu, Chun Wei, Yongyang Gong, Zirun Chen, Dejiang Yang, Heng Su & Tianxi Liu

To cite this article: Zihao Xu, Chun Wei, Yongyang Gong, Zirun Chen, Dejiang Yang, Heng Su & Tianxi Liu (2017) Efficient dispersion of carbon nanotube by synergistic effects of sisal cellulose nano-fiber and graphene oxide, Composite Interfaces, 24:3, 291-305, DOI: 10.1080/09276440.2016.1227655

To link to this article: https://doi.org/10.1080/09276440.2016.1227655

COMPOSITE INTERFACES, 2017
VOL. 24, NO. 3, 291–305
http://dx.doi.org/10.1080/09276440.2016.1227655

Taylor & Francis
Taylor & Francis Group

Efficient dispersion of carbon nanotube by synergistic effects of sisal cellulose nano-fiber and graphene oxide

Zihao Xu[a], Chun Wei[a,b,c], Yongyang Gong[a,b,c], Zirun Chen[a], Dejiang Yang[a], Heng Su[a] and Tianxi Liu[b,c]

[a]College of Materials Science and Engineering, Guilin University of Technology, Guilin, PR China; [b]Ministry-Province Jointly-Constructed Cultivation Base for State Key Laboratory of Processing for Non-Ferrous Metal and Featured Materials, Guilin, PR China; [c]Key Laboratory of New Processing Technology for Nonferrous Metals and Materials, Ministry of Education, Guilin, PR China

ABSTRACT

A highly flexible and conductive nanohybrid film based on multi-walled carbon nanotube (MWNT) was prepared using synergistic dispersion effects of nanosisal cellulose and graphene oxide (GO). The dispersion effect of MWNT was characterized using illustrative diagrams of different dispersions after centrifuge, transmission electron microscope, and Zeta potential, respectively. The results showed that 80 wt% MWNT was efficiently dispersed and formed a stable nanodispersion solution using 10 wt% cellulose nanofiber (CNF) and 10 wt% GO as dispersants. The conductivity and tensile strength of the CNF/GO/MWNT nanocomposite film were up to 1818.19 S/m and 25 MPa, respectively.

ARTICLE HISTORY
Received 20 May 2016
Accepted 19 August 2016

KEYWORDS
Nanocellulose; graphene oxide; carbon nanotube; synergistic dispersion; conductive film

1. Introduction

Cellulose is the most abundant renewable and green polymer in nature and is mainly produced through photosynthesis of plants. In recent years, growing pollution, the decline of petroleum, and coal reserves have inspired the application of renewable resources in medical and optical fields; the applications of cellulose gained increasing attention and development.[1,2] Cellulose nanofiber (CNF) is a linear nanomaterial with 5–30 nm in diameter and 100s or 1000s of nanometers in length. It has high elastic modulus, low thermal expansion coefficient, great flexibility, relative thermostabilization, and alterable optical appearance. These properties allow nanocellulose to be applied in reinforcement materials, biomaterial, drug delivery, membrane, and so on.[3–6] Furthermore, CNF also functions as a dispersion medium due to the hydrophobic site and hydrophilic functional groups over its surface.[7]

Graphene oxide (GO) is a 2-D lamellar nanomaterial derived from stripped oxidized graphite. Because of the strong oxidation, many oxygen-containing functional groups such as –OH, –COOH, and epoxy groups are generated, which enable GO to possess the great hydrophilicity. Hence, GO is stably dispersed in aqueous solutions. Moreover, GO has

CONTACT Chun Wei 1986024@glut.edu.cn

high specific surface area and numerous functional groups. These benefits of GO ensure its application in optoelectronics, biomedicine, analysis detection, and other scopes.[8–10]

Carbon nanotube (CNT) is a one-dimensional tubular nanomaterial that has excellent mechanical and electrical properties. It has been widely used in many fields including energy storage, biotechnology, and coatings.[11]

The advantageous properties of CNF, GO, and CNT materials have drawn the focus of many studies. For instance, CNF and crumpled graphene were utilized to fabricate a free-standing flexible nanopaper using a vacuum filtration method, resulting in the improvement of nanopaper stretchability from 6% to 100%.[12] Zheng et al. [13] fabricated an all solid-state super capacitor using hybrid aerogels consisting of CNF, reduced GO, and CNT, which exhibited a high specific capacitance (252 F g^{-1}) and remarkable cycle stability. Wang et al. [14] fabricated composite paper electrodes by coupling polypyrrole/GO on CNF via *in situ* polymerization, and the process was carried out for over 16,000 cycles. Wang et al. [15] combined the mechanically excellent NFC and functionalized few-walled CNT to produce hybrid nanofiber/nanotube aerogels; this composite material showed elastic mechanical behavior in combination with reversible electrical response and pressure sensing, which combined the concept of CNF and electrical functionality of CNT synergistically. Cao et al. [16] used a pressure-controlled aqueous extrusion process to assemble lithium titanate/CNT/cellulose nanofiber hybrid network film which was used as a lithium-ion battery (LIB) electrode. In the heterogeneous fibrous network of the hybrid film, CNF served as building skeleton and a biosourced binder, CNT/CNF layer was used as a lightweight current collector, and the network film had extremely good conductivity of 15.0 S/cm, and the LIB electrode showed very good high-rate cycling performance. Carlos [17] and co-author prepared stable aqueous colloidal suspensions of composite particles made of sigmacell cellulose and multi-walled carbon nanotubes (MWNTs). These suspensions were dried and redispersed in water. The adsorption ability of composite particles was used at cyclohexane–water interfaces, which demonstrated an original way of stabilizing oil-in-water Pickering emulsions, and the cyclohexane droplet diameters were easily tuned from 20 to 100 μm by adjusting the concentration of composite particles.

Despite the excellent properties of them, their weaknesses also exist, including one in CNT. The hydrophobic structure makes it difficult for CNT to uniformly disperse in solvents, particularly in water, which greatly limits its potential application in electronic materials and biological medicine.[18]

In this paper, homemade sisal CNF and GO functioned as dispersion agents to disperse MWNTs by mechanical agitation in water, and the dispersions were used for the preparation of CNF/GO/MWNT complexes. This method is more environment-friendly and efficient, which is differ from the old traditional method that adding surfactant [19] and acid treatment.[20] In the meantime, the optimized ratio of CNF to GO and the dispersion mechanism of the synergy between CNF and GO were discussed. Furthermore, a CNF/GO/MWNT conductive film was prepared and its conductive properties were studied. This work explores fields of application for natural nanocellulose in functional materials.

2. Experimental

2.1. Materials

Sisal fibers were obtained from Guangxi Sisal Corporation. Flake-like graphite (<20 μm) was purchased from ChenYang Graphite Co., Ltd., and used without further purification. MWNTs (5–15 μm length; 15–25 nm diameter), purified by acid treatment, were supplied by Shenzhen Nanotechnology Co., Ltd. Sodium hydroxide and sodium chloroacetate was obtained from Aladdin Industrial Corporation and Huihai Composite Material Co., Ltd (China). Other analytical reagents including sulfuric acid, hydrochloric acid, sodium nitrate, hydrogen peroxide, and potassium permanganate were purchased from Xilong Chemical Co., Ltd (China). The GO was homemade [21] and sisal cellulose microcrystalline (SCM) was also homemade.[22]

2.2. Preparation of sisal cellulose nano-fiber

About six grams of SCM was soaked in 18 mL of 5 wt% NaOH (aq) at room temperature for 30 min. The treated SP was then placed in a 500-mL three-neck flask and 0.553 g of NaOH, 1.848 g of sodium chloroacetate, and 120.46 mL of anhydrous ethanol were added. The mixture was refluxed at 75 °C in a water bath for 3 h. After the reaction, the product was placed in filter cloth and rinsed with deionized water to remove free reagents until it became neutral. The neutral product was then mixed with 1000 mL of deionized water to form a suspension with concentration reaching 0.5–0.6%. After that, the suspension was placed in a high-speed mixer by stirring and shearing for 10 min, until a transparent gel-like dispersion was formed. Eventually, the dispersion was centrifuged at 12,000 rpm for 5 min in order to remove the macrofibril, the CNF suspension (0.2%) was obtained, and –COOH group were grafted on its surface. Furthermore, CNF suspensions were dried in a dryer at the temperature of 60 °C, producing 3.43 g dried CNF for a yield of 57.2%.

2.3. Preparation of GO/MWNT dispersions

As shown in Figure 1(a), different amounts of oxidized graphite were added to 200-ml deionized water and dispersed with a homogenizer at a speed of 28,000 rpm for 30 min. Then the mixture was centrifuged at 12,000 rpm for 10 min to remove the aggregates. The obtained supernatants were used to disperse the MWNTs. After that, different amounts of MWNT were independently added to the GO dispersions at the mass ratios (GO to MWNT) of 20/80, 30/70, 40/60, 50/50, 60/40, 70/30, 80/20, and 90/10. The total mass was 0.3 g after the addition of water, and the mass was the same in the following experiments. Finally, these GO/MWNT dispersions were stirred in the high-speed mixer for 10 min to prepare the GO/MWNT dispersions.

2.4. Preparation of CNF/MWNT dispersions

As shown in Figure 1(b), different amounts of MWNT were independently added to CNF suspension (0.2%) with 200-ml deionized water to form mixtures with CNF/MWNT at mass ratios of 10/90, 20/80, 50/50, 80/20, and 90/10. The mixtures were then stirred in high-speed mixer for 10 min to prepare the CNF/MWNT dispersions.

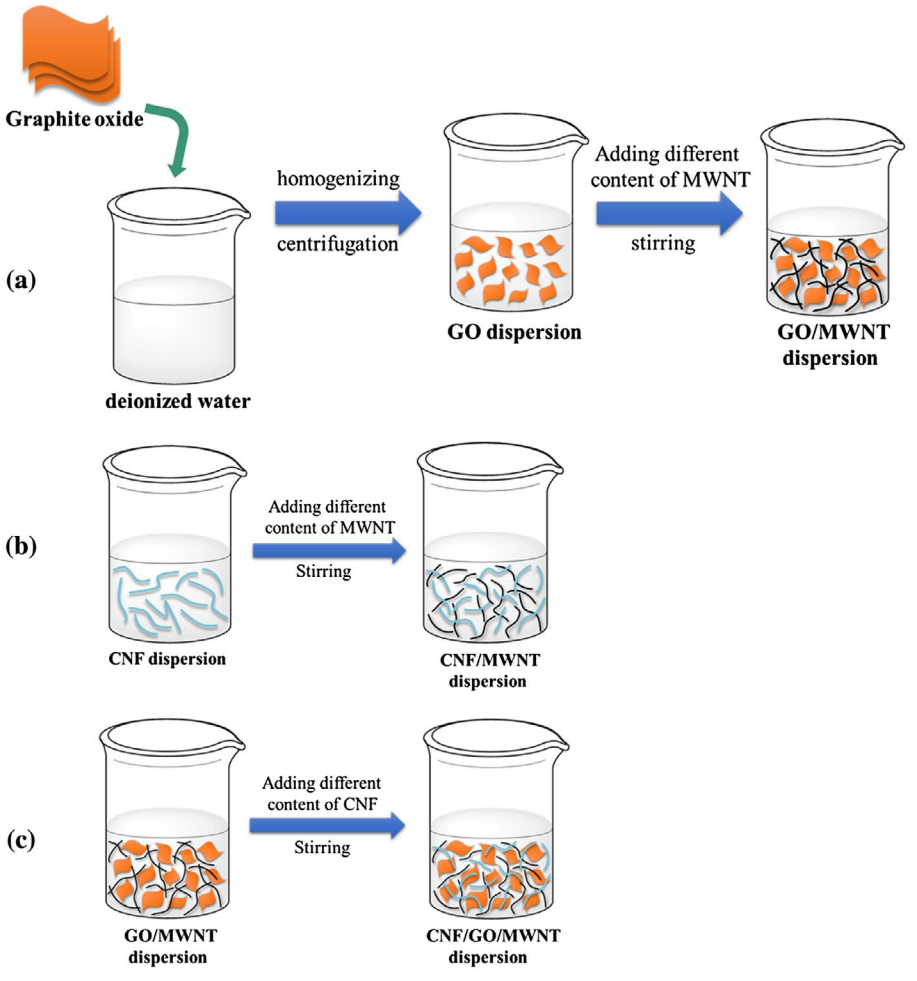

Figure 1. Schematic of fabrication process of (a) GO/MWNT dispersion, (b) CNF/MWNT dispersion, and (c) CNF/GO/MWNT dispersion.

2.5. Preparation of CNF/GO/MWNT dispersions

As shown in Figure 1(c), different amounts of CNF suspension (0.2%) were independently added to the prepared GO/MWNT dispersions to form the CNF/GO/MWNT mixtures, with which the total volume was 200 ml. The mass ratios of CNF/GO/MWNT were 10/10/80, 10/20/70, 20/10/70, and 30/10/60, respectively. These mixtures were then stirred in high-speed mixer for 10 min. The CNF/GO/MWNT dispersions were obtained.

2.6. Preparation of CNF/GO/MWNT conductive film

About 20 mL of the prepared CNF/GO/MWNT dispersion was placed on a filter membrane in a vacuum filtration device (filter membrane diameter: 47 mm; filter membrane pore size: 22 μm). A conductive film was formed by the vacuum filtration process. The film and filter membrane were dried at 60 °C for 6 h in an oven. Then, the film was stripped from the filter membrane with a pair of tweezers (see Figure 2).

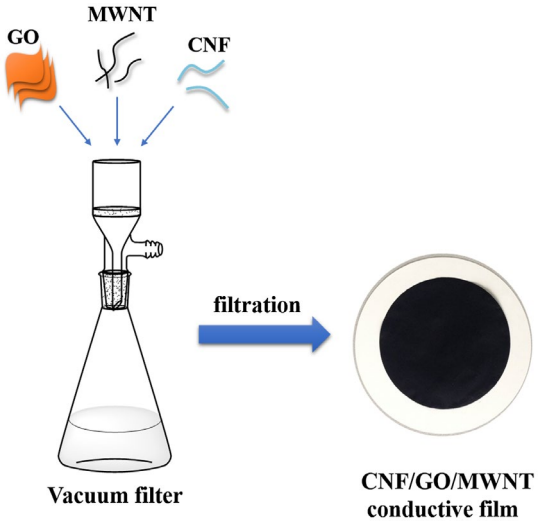

Figure 2. Schematic of fabrication process of CNF/GO/MWNT conductive film.

2.7. Analysis and characterizations

A JEOL JEM-2100F transmission electron microscope (TEM) was used to observe the morphology and structure of the dispersion at 200 kV. Drops of ca. 0.001 wt% which was prepared for dispersion were deposited onto copper net coated with carbon. These were negatively stained with 2 wt% uranyl acetate. An AJSM-6380 LA scanning electron microscope was used to characterize the surface morphology of conductive films, which were coated with a thin layer of gold. A Q800 dynamic mechanical analyzer (DMA, TA Corporation, United States) was used to measure the stress–strain curves (5 N/min, 25 °C) of the film, and the specimen size was 18 × 6.02 × 0.02 mm. The functional groups of the MWNT, GO/MWNT, and CNF/GO/MWNT were analyzed with a Nexus 470 Fourier transform infrared spectroscope (FT-IR, Nicolet) at a resolution of 4 cm^{-1} over the range of 4000–500 cm^{-1}, and all samples were carried out after strict drying. The stability of the GO/MWNT, CNF/MWNT, and CNF/GO/MWNT dispersions was characterized with a ZS90 Zeta potential analyzer (Malvern) with solid content of 0.5 mg/ml at 25 °C at pH 7.0. Electrical resistivity of the conductive film was measured with a four probe method by KDY-1A tester (Kunde Corporation, China), and the test procedure referred to previous research.[23] The aforementioned stirring processes were performed with a JK-818 mixer.

3. Results and discussion

3.1. Dispersion characterization

The GO/MWNT, CNF/MWNT, and CNF/GO/MWNT dispersion were centrifuged at 8000 rpm for 5 min, and their supernatants were obtained to observe their degree of dispersion.

The prepared GO/MWNT dispersion with mass ratios of 20/80, 30/70, 40/60, 50/50, 60/40, 70/30, 80/20, and 90/10 is illustrated in Figure 3. When the mass ratio of GO was

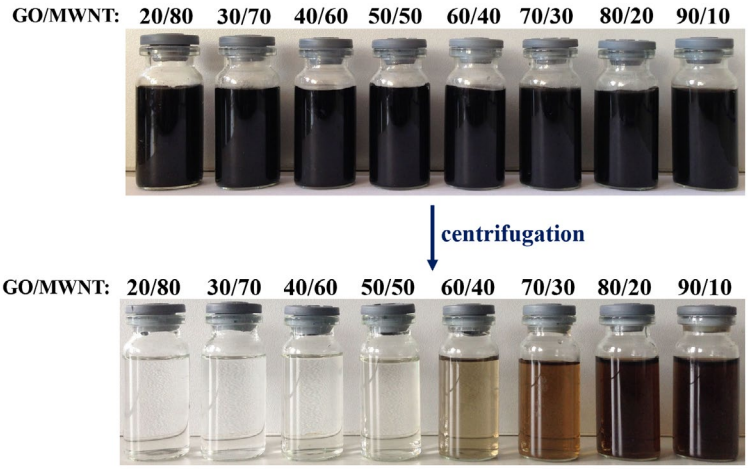

Figure 3. Digital picture of the GO/MWNT dispersion before and after centrifugation.

lower than 60%, the centrifuged supernatants were colorless and transparent, indicating that the MWNT precipitated after the centrifugation and dispersion failed. In contrast, when the mass ratio was higher than 60%, the color of the centrifuged supernatants showed a general trend of evolution from shallow to deep, indicating that the MWNT was partially dispersed by the 60 wt% of GO. The dispersion effect was more significant as the content of GO increased.

The above phenomenon was similar to previously mentioned references. Zhang et al. have studied that when the initial proportion of MWNT to GO was 2:1, excessive MWNT got tangled and twisted on the GO sheets, thus leading to serious aggregation. When the initial proportion of MWNT to GO was 1:2, the MWNT was diluted and after a dynamic equilibrium process, due to sonication, the stable dispersion of GO/MWNT dispersion was formed by π-stacking interaction between MWNT and GO.[24] Qiu et al. used single-walled CNTs to blend with GO, and found that sonicating a mixture of GO dispersion and CNT powder (0.05 wt%) resulted in the formation of a black and stable suspension. Then the dissolved CNTs was associated with the GO through π–π stacking interaction between the delocalized electrons in both the aromatic regions of GO sheets and CNTs.[25] Dong et al. also studied the interaction between CNTs and GO. A stable aqueous dispersion of the CNTs and GO nano-sheets was produced by sonication mixing without assistance of any surfactant; the reason was that GO nano-sheets were wrapped onto the CNTs bundle to form a core-shell structure through π–π stacking.[26] All of these studies further indicated that the interaction of CNTs with GO was possible and it stabilized the CNTs dispersion via π-stacking between the multiple aromatic regions of GO sheets and CNTs. The dispersion mechanism is illustrated in detail in Figure 4.

The CNF/MWNT dispersion systems are illustrated in Figure 5. The mass ratios of CNF/MWNT were 10/90, 20/80, 50/50, 80/20, and 90/10. It was demonstrated that when the content of CNF was 10 wt%, the color of the centrifugated supernatant was lighter in comparison to the uncentrifuged supernatant. When the content of CNF exceeded 20 wt%, the color of the dispersion solutions remained essentially unchanged before and after the

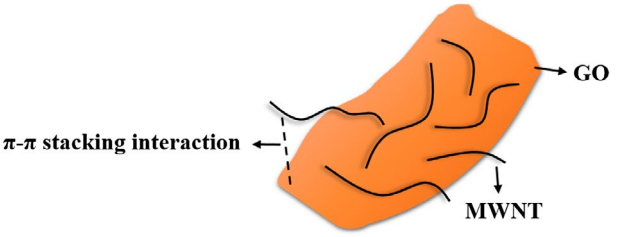

Figure 4. The dispersing mechanism of GO/MWNT dispersion.

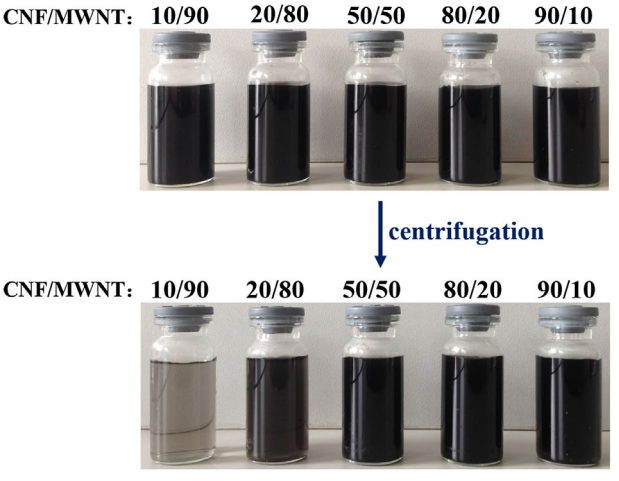

Figure 5. Digital picture of the CNF/MWNT dispersion before and after centrifugation.

centrifugation, indicating that the content of CNF over 20 wt%, CNF could effectively disperse the MWNT.

The dispersion effect of the prepared CNF was attributed to two reasons: Firstly, the surface of CNFs in this experiment contained some carboxyl functional groups over themselves. Therefore, the electrostatic repulsion was formed between the CNF/MWNT nano aggregates, resulting in the dispersion of CNF/MWNT.[27] Secondly, CNF is believed to be a hydrophilic substance due to the presence of polar groups like hydroxyl groups. However, there are some hydrophobic faces also exist because of non-polar functional groups such as –CH moieties on its surface. Due to the presence of both polar –OH groups and non-polar –CH moieties, CNF is considered to be amphiphilic.[28] While MWNT is a hydrophobic tubular and linear substance, the CNF would interact with MWNT through hydrophobic–hydrophobic interaction between their surfaces (Figure 6). Consequently, the MWNT was well dispersed by the interaction between them.[29]

The CNF/GO/MWNT (10/10/80 wt%) dispersion systems are illustrated in Figure 7. As can be seen, the dispersion system was black and homogeneous both before and after the centrifugation. Although there was a small amount of CNF and GO in system, it dispersed MWNT effectively. It was reasonable to conclude that there was a synergetic effect between the CNF and GO with the dispersion of the MWNT.

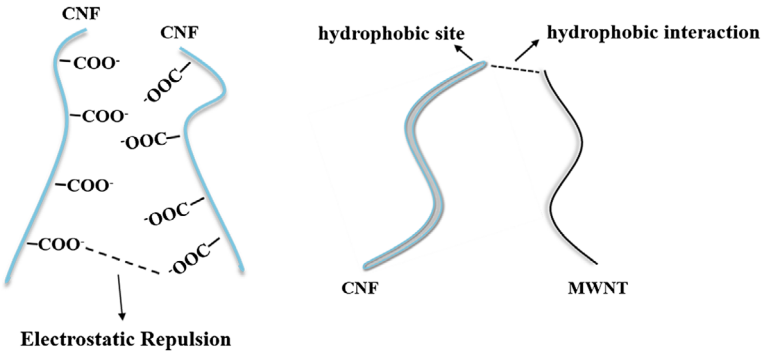

Figure 6. The dispersing mechanism of CNF/MWNT dispersion.

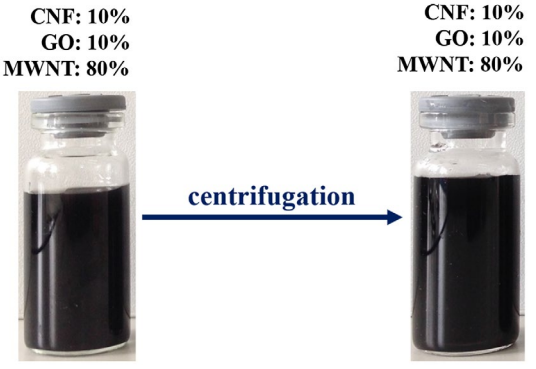

Figure 7. Digital picture of the CNF/GO/MWNT dispersion before and after centrifugation.

This synergetic effect could be ascribed to the great interfacial interactions between the GO and CNF. The CNF bridged the GO sheets with the hydrogen bonds formed between –OH over the CNF and the oxygen-containing functional groups over the GO sheets.[30] The MWNT not only interacted with the GO through π-stacking, but was also repulsed by the CNF via their electrostatic repulsion and the hydrophobic interaction between hydrophobic functional groups, which resulted in a better dispersion of the MWNT (Figure 8).

3.2. FTIR analysis

The infrared spectra of MWNT, GO/MWNT, and CNF/GO/MWNT complexes are illustrated in Figure 9.

Strong absorption peaks were not observed in the spectrum of the MWNT (curve A in Figure 9), which indicated that functional groups were rare on the surface of the MWNT. The weak absorption peak at 1384 cm^{-1} could be attributed to impure peaks of potassium bromide, because it was used as a medium to load samples in this experiment, and the same peaks were also found in other infrared spectra.

In the spectrum of the GO/MWNT complexes (curve B in Figure 9), the strong absorption peak was at 3472 cm^{-1} which corresponded to the stretching vibration of –OH. The

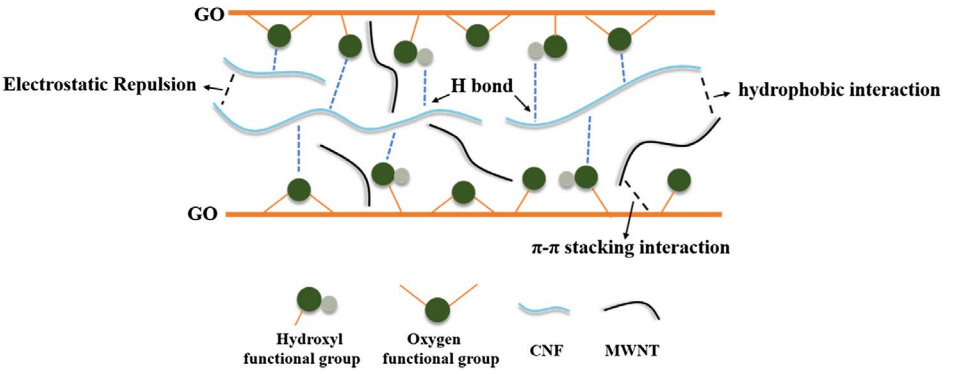

Figure 8. The dispersing mechanism of CNF/GO/MWNT dispersion.

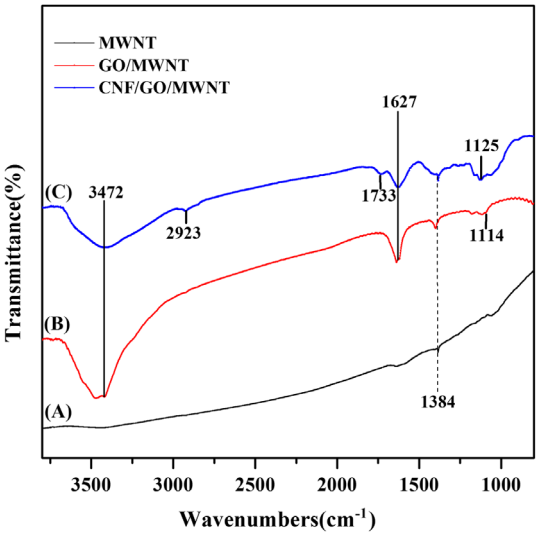

Figure 9. FTIR spectra of (A) MWNT, (B) GO/MWNT complexes, (C)CNF/GO/MWNT complexes.

absorption band at 1627 cm^{-1} was attributed to the bending vibration of C–OH, which indicated the presence of carbonyl groups. Additionally, the vibration absorption peak of C–O–C group was also observed at 1114 cm^{-1}. These oxygen-containing functional groups were abundant on GO, but did not appear on MWNT, so this indicated the presence of GO in the GO/MWNT complexes.

In the spectrum of the CNF/GO/MWNT complexes (curve C in Figure 9), in addition to the two peaks corresponding to C–OH and –OH, the stretching vibration of C–H of methyl and methylene in the CNF was detected at 2923 cm^{-1}. Moreover, the peak at 1733 cm^{-1} corresponded to the vibration of –COOH on CNF, this proved the existence of the carboxyl as was mentioned previously. Moreover, it was found that the absorption peak was at 1125 cm^{-1}, which was attributed to the C–O–C antisymmetric vibration of glucosides on CNF. From the results, the existence of each substance in the CNF/GO/MWNT complexes was confirmed.

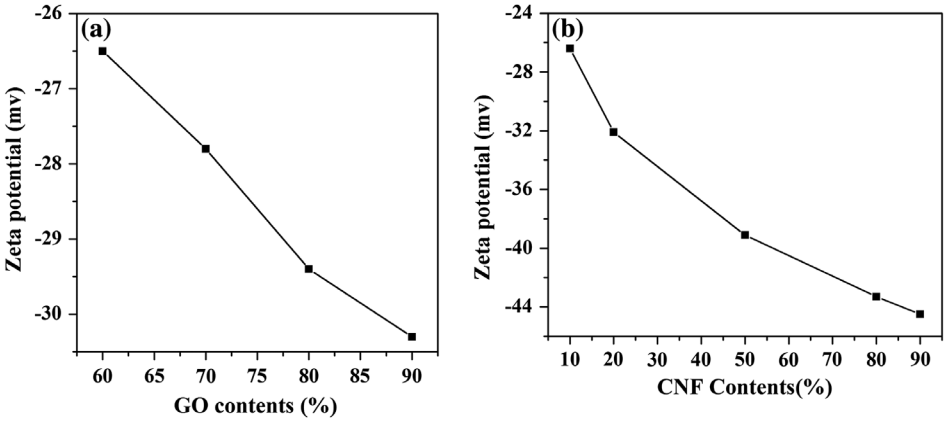

Figure 10. Zeta potential of (a) GO/MWNT dispersion, (b) CNF/MWNT dispersion.

3.3. Zeta potential analysis

To understand the stability of dispersions, Zeta potential was performed, and potential value that was more positive than +30 mV or more negative than −30 mV indicated stability. As can be seen in Figure 10(a), when the content of GO in the GO/MWNT dispersion was 60 wt%, the value of Zeta potential was −26.5 mV, which indicated that the system was relatively stable. When the GO content was 90 wt%, the Zeta potential was −30.3 mV and the system was even more stable. The Zeta potential gradually decreased and stability increased with the increase in the GO content, which demonstrated that the MWNT was stable and effectively dispersed by the content of GO over 60 wt%.

The CNF/MWNT dispersion system is shown in Figure 10(b).It shows that when CNF content was 10 wt%, the value of the Zeta potential was −26.4 mV, and the system was relatively stable. When the CNF content was 20 wt%, the Zeta potential was −32.1 mV, which illustrated the system was stable in water. This indicated that the CNF content had a positive effect on the stability of the CNF/MWNT dispersion. It was confirmed that MWNT was well dispersed when the content of CNF was over 20 wt%.

The Zeta potential of the CNF/GO/MWNT (10/10/80 wt%) dispersion system was as low as −35.2 mV, which indicated that the system was quite stable. Compared to the mass ratio of 90/10 GO/MWNT dispersion and 20/80 CNF/MWNT dispersion, the Zeta potential value was decreased further and the content of both GO and CNF was as low as 10 wt%. Based on our findings, it proved the synergistic effect of CNF/GO on the dispersion of the MWNT based on a stability perspective.

3.4. TEM characterization

TEM images of the GO/MWNT (70/30 wt%) complexes are illustrated in Figure 11(a) and (b). The MWNT was inserted in GO and instead of tangling and aggregating on the sheet of GO, it uniformly dispersed between the GO sheets and formed a stable dispersion. This further illustrated that the MWNT was effectively dispersed in the GO when the content was over 60 wt%.

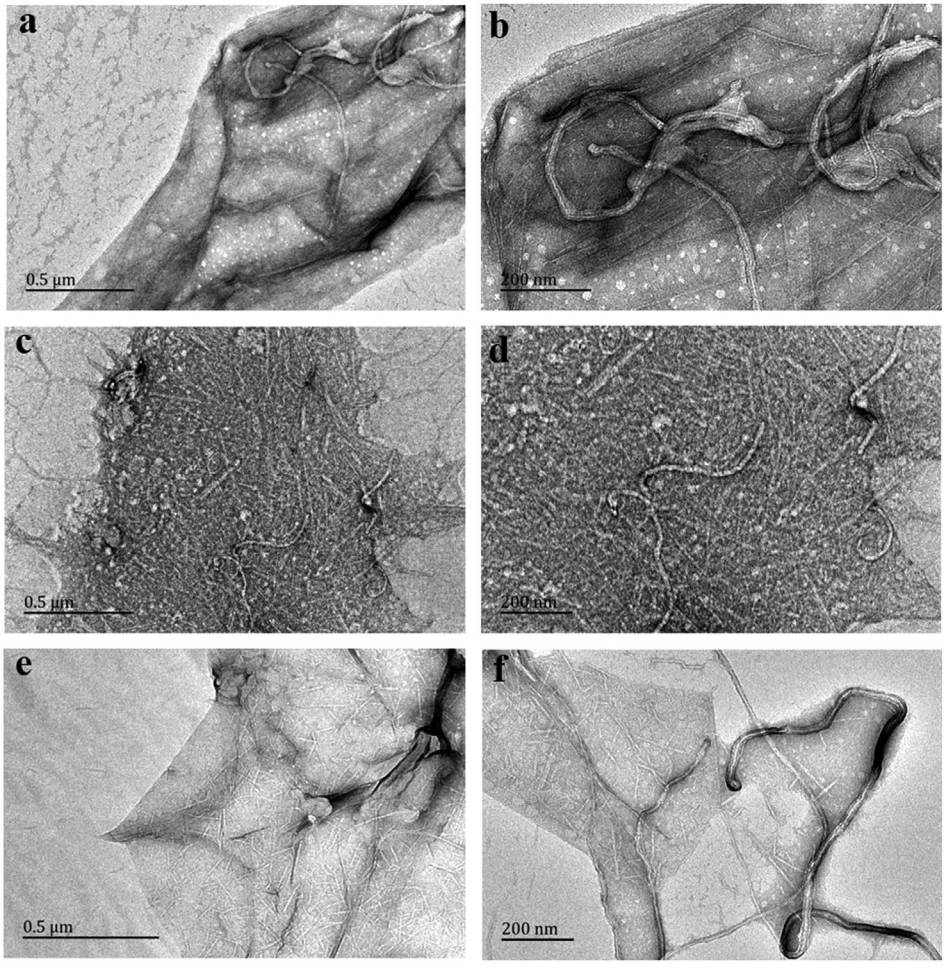

Figure 11. TEM images of the (a, b) 70/30 GO/MWNT complexes, (c, d) 20/80 CNF/MWNT complexes, (e, f) 10/10/80 CNF/GO/MWNT complexes.

TEM images of CNF/MWNT (20/80 wt%) complexes are shown in Figure 11(c) and (d). The MWNT did not appeared in the formation of aggregation, instead it was in the singly rooted form, while CNF was also uniformly separated around MWNT. These indicated that MWNT was uniformly dispersed via the electrostatic repulsion and hydrophobic interaction with CNF, which verified the dispersion and stability function of the CNF, as discussed earlier.

TEM images of the CNF/GO/MWNT (10/10/80 wt%) complexes in Figure 11(e) and (f) illustrated that when the contents of the CNF and GO were each decreased to 10 wt%, the CNF and MWNT were uniformly dispersed between the GO sheets to form a single chain without aggregation. It was believed that the CNF and GO would interact with each other by hydrogen bonding. Through the electrostatic repulsion between the CNF, π-stacking effect between the GO and MWNT, and repulsion interaction between the hydrophobic groups of the CNF and MWNT, the system was uniformly dispersed. The synergistic effects of the CNF and GO were reflected by these complex interactions.

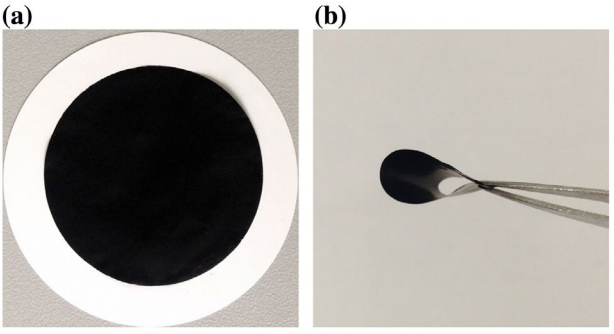

Figure 12. (a) Digital picture of the 10/10/80 CNF/GO/MWNT conductive film, (b) Flexibility of the 10/10/80 CNF/GO/MWNT conductive film.

3.5. The electric resistivity and mechanical properties

The 10/10/80 CNF/GO/MWNT conductive film is shown in Figure 12(a), which was smooth and uniform. Additionally, the prepared film also demonstrated great flexibility, as shown in Figure 12(b). Then, in order to study synergistic effect clearly, 10/10/80 CNF/GO/MWNT, 20/80 CNF/MWNT, and 60/40 GO/MWNT films were measured with 'stress-strain' and conductivity, and due to 20 wt% GO, 60/40 GO/MWNT film could not effectively disperse MWNT. In these results, as shown in Figure 13(a), the conductivity of the films increased with the addition of MWNT. This was because of the formation of more conductive path with the increase in MWNT. When the content of MWNT was similar, the conductivity of CNF/GO/MWNT film reached 1818.19 S/m which was higher than the CNF/MWNT film (1527.72 S/m). This indicated that a more conductive path existed in the CNF/GO/MWNT film. The CNF/GO was better than only CNF in aspect of dispersing MWNT, which reflected the synergistic effect between CNF and GO. As shown in Figure 13(b), like the analysis above, the tensile strength of CNF/GO/MWNT film attained 25 MPa, which was stronger than the CNF/MWNT (18.86 MPa) and GO/MWNT (9.31 MPa) film. This was attributed to the better interface interaction between CNF/GO and MWNT. This also illustrated that MWNT was dispersed more uniformly by CNF/GO than CNF and GO, which confirmed the synergistic effect between CNF and GO further from another perspective.

In order to further study the interfacial interaction of the CNF, GO and MWNT, the surfaces of conductive films were observed by SEM. As shown in Figure 14(a) (60/40 GO/MWNT), the MWNTs exhibited a hollow tubular structures with diameters of approximately 20 nm, and excessive GO sheets were bestrewed with a small number of MWNTs leading to the low conductivity of film. This verified that over 60 wt% GO could disperse MWNTs. In Figure 14(b) (20/80 CNF/MWNT), MWNTs dispersed uniformly instead of serious tangling, and the CNF was separated around the MWNTs, whichindicated that MWNTs were dispersed effectively by CNF. While the diameter of CNF was about 32.5 nm due to the aggregation from the hydrogen-bond interaction during the film-forming process. When adding the GO into CNF/MWNT complexes, as can be seen in Figure 14(c) (10/10/80 CNF/GO/MWNT), CNF and MWNTs were inserted in the GO sheets, and the MWNTs were dispersed more uniformly without aggregation. These illustrated that MWNTs could be well dispersed by the synergistic effects of the CNF and GO, giving materials the better performance.

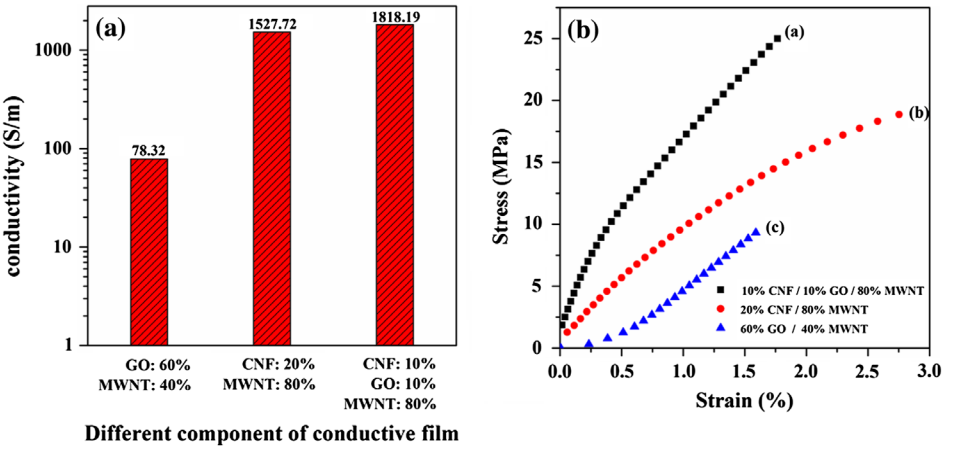

Figure 13. Conductivity (a) and typical stress–strain curve, (b) of 10/10/80 CNF/GO/MWNT conductive film, 20/80 CNF/MWNT conductive film, 60/40 GO/MWNT conductive film.

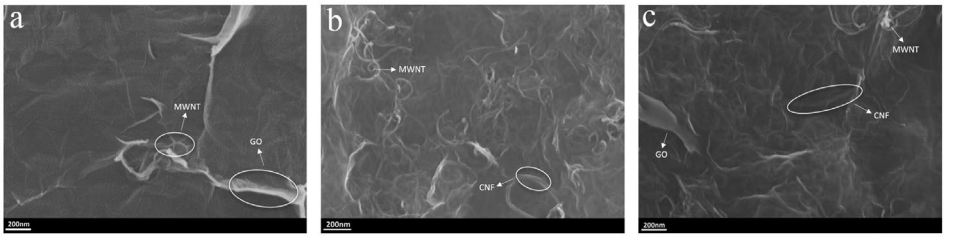

Figure 14. FESEM images of (a) 60/40 GO/MWNT conductive film, (b) 20/80 CNF/MWNT conductive film, (c) 10/10/80 CNF/GO/MWNT conductive film.

4. Conclusions

In summary, with the use of nontoxic, green CNF, and advanced carbon functional materials GO as the dispersion medium and through the synergistic effects of CNF and GO, MWNT was successfully dispersed. The results showed that CNF (over 20 wt%) effectively dispersed MWNT in the absence of GO, and GO (over 60%) effectively dispersed MWNT in the absence of CNF. However, the mixture of 10 wt% CNF and 10 wt% GO also efficiently dispersed and stabilized MWNT through their synergistic effects due to the hydrogen bonding between CNF and GO. The conductivity of the film produced from the 10/10/80 CNF/GO/MWNT dispersion was 1818.2 /m with tensile strength of 25 MPa which were both higher than 20/80 CNF/MWNT and 60/40 GO/MWNT conductive films. It is demonstrated that the synergy between CNF and GO is beneficial for the dispersion of CNTs, which is applicable for the preparation of nanoconductive films. These films could find various applications in bendable electronics, electromagnetic shielding, and electromagnetic pulse protection.

Disclosure statement

No potential conflict of interest was reported by the authors.

Funding

The authors would like to acknowledge the National Natural Science Foundation of China [grant number 21264005, 51263005]; Guangxi Natural Science Foundation of China [grant number 2014GXNSFAA118321]; Foundation of Guangxi Ministry-Province Jointly-Constructed Cultivation Base for State Key Laboratory of Processing for Non-ferrous Metal and Featured Materials [grant number 13AA-6].

References

[1] Saba N, Tahir PM, Jawaid M. A review on potentiality of nano filler/natural fiber filled polymer hybrid Composites. Polymers. 2014;6:2247–2273.
[2] Giri J, Adhikari R. A brief review on extraction of nanocellulose and its application. Bibechana. 2012;9:81–87.
[3] Shen F, Zhu H, Luo W, et al. Chemically crushed wood cellulose fiber towards high-performance sodium-ion batteries. ACS Appl. Mat. Interfaces. 2015;7:23291–23296.
[4] Qiu X, Hu S. "Smart" materials based on cellulose: a review of the preparations, properties, and applications. Materials. 2013;6:738–781.
[5] Siró I, Plackett D. Microfibrillated cellulose and new nanocomposite materials: a review. Cellulose. 2010;17:459–494.
[6] Moon RJ, Martini A, Nairn J, et al. Cellulose nanomaterials review: structure, properties and nanocomposites. Chem. Soc. Rev. 2011;40:3941–3994.
[7] Kalashnikova I, Bizot H, Cathala B, et al. Modulation of cellulose nanocrystals amphiphilic properties to stabilize oil/water interface. Biomacromolecules. 2011;13:267–275.
[8] Dreyer DR, Park S, Bielawski CW, et al. The chemistry of graphene oxide. Chem. Soc. Rev. 2010;39:228–240.
[9] Zhu Y, Murali S, Cai W, et al. Graphene and graphene oxide: synthesis, properties, and applications. Adv. Mater. 2010;22:3906–3924.
[10] Tang Y, He Z, Mosseler JA, et al. Production of highly electro-conductive cellulosic paper via surface coating of carbon nanotube/graphene oxide nanocomposites using nanocrystalline cellulose as a binder. Cellulose. 2014;21:4569–4581.
[11] Ahir S, Huang Y, Terentjev E. Polymers with aligned carbon nanotubes: active composite materials. Polymer. 2008;49:3841–3854.
[12] Yan C, Wang J, Kang W, et al. Highly stretchable piezoresistive graphene–nanocellulose nanopaper for strain sensors. Adv. Mater. 2014;26:2022–2027.
[13] Zheng Q, Cai Z, Ma Z, et al. Cellulose nanofibril/reduced graphene oxide/carbon nanotube hybrid aerogels for highly flexible and all-solid-state supercapacitors. ACS Appl. Mat. Interfaces. 2015;7:3263–3271.
[14] Wang Z, Tammela P, Strømme M, et al. Nanocellulose coupled flexible polypyrrole@graphene oxide composite paper electrodes with high volumetric capacitance. Nanoscale. 2015;7:3418–3423.
[15] Wang M, Anoshkin IV, Nasibulin AG, et al. Modifying native nanocellulose aerogels with carbon nanotubes for mechanoresponsive conductivity and pressure sensing. Adv. Mater. 2013;25:2428–2432.
[16] Cao S, Feng X, Song Y, et al. Integrated fast assembly of free-standing lithium titanate/carbon nanotube/cellulose nanofiber hybrid network film as flexible paper-electrode for lithium-ion batteries. ACS Appl. Mat. Interfaces. 2015;7:10695–10701.
[17] Avendano C, Brun N, Fontaine O, et al. Multiwalled carbon nanotube/cellulose composite: from aqueous dispersions to pickering emulsions. Langmuir. 2016;32:3907–3916.
[18] Huang Y, Terentjev E. Dispersion and rheology of carbon nanotubes in polymers. Int. J. Mater. Form. 2008;1:63–74.
[19] Vaisman L, Wagner HD, Marom G. The role of surfactants in dispersion of carbon nanotubes. Adv. Colloid Interface Sci. 2006;128–130:37–46.

[20] Saito T, Matsushige K, Tanaka K. Chemical treatment and modification of multi-walled carbon nanotubes. Physica B. 2002;323:280–283.
[21] Hummers WS Jr, Offeman RE. Preparation of graphitic oxide. J. Am. Chem. Soc. 1958;80:1339–1339.
[22] Li X, Liu H, Wei C, et al. Extraction and characterization of cellulose microcrystal from sisal fibers. Polym. Mater. Sci. Eng. 2012;28:160–162, 166.
[23] Pei S, Zhao J, Du J, et al. Direct reduction of graphene oxide films into highly conductive and flexible graphene films by hydrohalic acids. Carbon. 2010;48:4466–4474.
[24] Zhang C, Ren L, Wang X, et al. Graphene oxide-assisted dispersion of pristine multiwalled carbon nanotubes in aqueous media. J. Phys. Chem. C. 2010;114:11435–11440.
[25] Qiu L, Yang X, Gou X, et al. Dispersing carbon nanotubes with graphene oxide in water and synergistic effects between graphene derivatives. Chem. A Eur. J. 2010;16:10653–10658.
[26] Dong X, Xing G, Chan-Park MB, et al. The formation of a carbon nanotube–graphene oxide core–shell structure and its possible applications. Carbon. 2011;49:5071–5078.
[27] Fujisawa S, Okita Y, Fukuzumi H, et al. Preparation and characterization of TEMPO-oxidized cellulose nanofibril films with free carboxyl groups. Carbohydr. Polym. 2011;84:579–583.
[28] Li Y, Zhu H, Shen F, et al. Nanocellulose as green dispersant for two-dimensional energy materials. Nano Energy. 2015;13:346–354.
[29] Pratt LR, Chandler D. Theory of the hydrophobic effect. J. Chem. Phys. 1977;67:3683–3704.
[30] Li Y, Zhu H, Zhu S, et al. Hybridizing wood cellulose and graphene oxide toward high-performance fibers. NPG Asia Mater. 2015;7:e150.